Seasonal growth and calcification of three species of crustose coralline algae in Moorea, French Polynesia

Camille Vizon, Laura Lagourgue, Claude E Payri, Maggy M Nugues

▶ **To cite this version:**

Camille Vizon, Laura Lagourgue, Claude E Payri, Maggy M Nugues. Seasonal growth and calcification of three species of crustose coralline algae in Moorea, French Polynesia. Marine Ecology Progress Series, 2024, 739, pp.31-48. 10.3354/meps14626 . hal-04704663

HAL Id: hal-04704663
https://hal.science/hal-04704663v1

Submitted on 21 Sep 2024

HAL is a multi-disciplinary open access archive for the deposit and dissemination of scientific research documents, whether they are published or not. The documents may come from teaching and research institutions in France or abroad, or from public or private research centers.

L'archive ouverte pluridisciplinaire **HAL**, est destinée au dépôt et à la diffusion de documents scientifiques de niveau recherche, publiés ou non, émanant des établissements d'enseignement et de recherche français ou étrangers, des laboratoires publics ou privés.

Distributed under a Creative Commons Attribution 4.0 International License

Vol. 739: 31–48, 2024
https://doi.org/10.3354/meps14626

MARINE ECOLOGY PROGRESS SERIES
Mar Ecol Prog Ser

Published July 4

Check for updates

OPEN ACCESS CC BY

Seasonal growth and calcification of three species of crustose coralline algae in Moorea, French Polynesia

Camille Vizon[1,*], Laura Lagourgue[2], Claude E. Payri[2], Maggy M. Nugues[1,3]

[1]PSL Université Paris: EPHE-UPVD-CNRS, UAR 3278 CRIOBE, Université de Perpignan, 66860 Perpignan, France
[2]UMR 9220 ENTROPIE, 'Ecologie Marine Tropicale des Océans Pacifique et Indien' (IRD, CNRS, Université de La Réunion, Université de la Nouvelle-Calédonie), IRD, 98848 Nouméa, New Caledonia
[3]Laboratoire d'Excellence Corail, 66860 Perpignan, France

ABSTRACT: Crustose coralline algae (CCA) play a critical role in the ecology and resilience of coral reefs by contributing to reef carbonate production and facilitating coral recruitment. However, little is known about their rates of *in situ* growth and calcification, particularly at the species level. To investigate the spatial and seasonal dynamics of CCA growth and calcification, we deployed CCA fragments embedded within epoxy rings at 3 mo intervals over 15 mo across 2 reef habitats in Moorea (French Polynesia). We studied 3 species differing in their microhabitat preferences (exposed, subcryptic and cryptic). Annual net calcification rates were highest in the exposed species *Porolithon* cf. *onkodes* (0.51 g $CaCO_3$ cm^{-2} yr^{-1}), intermediate in the subcryptic species *Neogoniolithon* cf. *megalocystum* (0.16 g $CaCO_3$ cm^{-2} yr^{-1}) and lowest in the cryptic species *Lithophyllum* sp. (0.03 g $CaCO_3$ cm^{-2} yr^{-1}). Growth and/or calcification rates differed between time intervals for all species. However, no consistent seasonal pattern was observed. *P.* cf. *onkodes* and *N.* cf. *megalocystum* had higher marginal growth rates at the fore reef habitat relative to the back reef habitat. This difference coincided with a lower occurrence of epiphytes on their crusts in the fore reef, suggesting that species interaction may be an important spatial driver of CCA growth. Our results show that CCA growth and calcification is species-specific and spatially and temporally variable. They highlight the need to consider subcryptic and cryptic CCA in reef carbonate budgets and provide important baseline information to understand how CCA communities are responding to environmental changes.

KEY WORDS: Crustose coralline algae · Calcification · Growth · Mortality · Bleaching · Seasonal · Moorea

1. INTRODUCTION

Coralline algae are calcareous red algae that belong to the orders Corallinales, Corallinapetrales, Hapalidiales and Sporolithales and are common in the euphotic zone of many benthic habitats (Steneck 1986, Schubert et al. 2020). Crustose (i.e. nongeniculate) coralline algae (CCA) play a critical role in the ecology of coral reefs. They contribute to reef resilience by providing settlement cues and hard substrata for corals and many benthic invertebrates (Morse et al. 1988, Heyward & Negri 1999, Harrington et al. 2004, Nelson 2009, Gómez-Lemos et al. 2018, Jorissen et al. 2021), whilst suppressing the recruitment and growth of macroalgae that would otherwise be harmful to corals (Vermeij et al. 2011, Gómez-Lemos & Diaz-Pulido 2017). After major disturbances, the rapid growth of CCA on dead corals may be pivotal in facilitating coral recruitment, leading to enhanced recovery of damaged reefs (Birrell et al. 2008, Perry & Morgan 2017). Together with scleractinian corals, CCA are also considered as locally important framework builders and carbonate producers (Steneck & Adey 1976, Payri 1997, Rasser & Riegl 2002, Gherardi & Bo-

*Corresponding author: camille.vi@hotmail.fr

© The authors 2024. Open Access under Creative Commons by Attribution Licence. Use, distribution and reproduction are unrestricted. Authors and original publication must be credited.

Publisher: Inter-Research · www.int-res.com

sence 2005). They can account for large proportions of coral reef carbonate production, especially following major disturbances such as mass coral bleaching events (Perry & Morgan 2017, Courtney et al. 2018, 2022). Under certain conditions, they can match or even exceed the contribution of corals to coral reef carbonate production (Cornwall et al. 2023).

Despite the ubiquity and ecological importance of CCA, knowledge on their ecology and the factors that drive their growth and calcification rates is seriously lacking, particularly at the species level. Measurements of individual CCA calcification rates are essential for understanding their contribution to the reef framework and carbonate budgets (Browne et al. 2021, Cornwall et al. 2023). However, CCA are often considered as a single functional group (Deinhart et al. 2022). Their identification at the species and even genus level based solely on morphology is challenging (Caragnano et al. 2018, Gabrielson et al. 2018), and sampling in the field is rarely coupled with molecular identification. CCA typically grow on both light-exposed and cryptic (i.e. shaded) reef surfaces. Thick encrusting coralline algae can be a prominent feature of tropical exposed reef crest and upper reef slope habitats and contribute substantially to reef development (Bak 1976, Adey 1978, MacIntyre 1997, Montaggioni et al. 1997, Teichert et al. 2020). Calcified algae also comprise a significant proportion of many coral reef cryptic assemblages (Kornder et al. 2021). Cryptic encrusting assemblages are important carbonate producers, that, under certain conditions, can deposit calcium carbonate at rates equal to those of their exposed counterparts (Mallela 2007, Morgan & Kench 2017). However, most of the existing research on individual CCA species have examined the growth and calcification of exposed species (Matsuda 1989, Lewis et al. 2017, Tâmega & Figueiredo 2019). Therefore, measurements of growth and calcification of cryptic calcifying algae are needed to assess their contribution to reef carbonate production (Cornwall et al. 2023).

The growth and calcification of CCA can be affected by a number of environmental and biological parameters, such as temperature (Ichiki et al. 2001, Martin et al. 2006, Short et al. 2015), light intensity (Littler 1973, Bessell-Browne et al. 2017, Morgan & Kench 2017), pH (Kuffner et al. 2008, Martin & Gattuso 2009, Diaz-Pulido et al. 2012, Martin et al. 2013), turbidity (Goh et al. 2021), sediment deposition (Kendrick 1991, Fabricius & De'ath 2001, Mallela 2013), nutrient loading (Tanaka et al. 2017), competition (Matsuda 1989, Short et al. 2014) and herbivory (Steneck & Adey 1976, Steneck et al. 1991, Figueiredo 1997). To date, most studies have relied on single experimental deployments and have rarely examined the role of seasonality on CCA growth and calcification. In general, CCA grow faster in summer than in winter (Adey 1970, Payri 1997, Blake & Maggs 2003, Martin et al. 2006, Kamenos & Law 2010, Burdett et al. 2011). However, this trend can vary, such as during prolonged heating events (Short et al. 2015, Tâmega & Figueiredo 2019). *In situ* seasonal studies comprising multiple experimental deployments provide important first steps towards understanding how naturally occurring communities of CCA respond to environmental changes.

Baseline information on CCA *in situ* seasonal growth and calcification is particularly lacking in the South Pacific. To date, only 1 *in situ* study (Payri 1997) has been carried out in this region. In the present study, we examined the spatio-temporal variation in rates of growth and calcification of 3 CCA species in Moorea (French Polynesia). This study was conducted in 2 distinct reef habitats (back reef and fore reef). All 3 CCA species inhabited both habitats, but differed in their microhabitat preferences (i.e. exposed, subcryptic, cryptic). Species identification was based on morphological observations and genetic characterisation. Since increased irradiance generally enhances CCA growth (Payri et al. 2001), we hypothesised that growth and calcification rates would be highest in the exposed species, intermediate in the subcryptic species and lowest in the cryptic species, and that, based on previous temporal studies, maximum seasonal growth and calcification rates would occur over the summer season.

2. MATERIALS AND METHODS

2.1. Study sites and species

We studied CCA growth and calcification at 2 sites (17° 28' 52.7" S, 149° 50' 55.62" W and 17° 28' 47.2" S, 149° 51' 06.8" W) representing 2 reef habitats (back reef and fore reef, respectively) during 5 ca. 3 mo time periods, from July 2021 to October 2022, on the island of Moorea, French Polynesia (Fig. 1). Moorea has a moist tropical climate divided into 2 distinct austral seasons: a cool, relatively dry season (approximately May to October) and a hot rainy season (approximately November to April), although strong interannual variations can occur, especially in recent decades. We refer to the 5 time periods as winter 2021 (July to October), spring 2021 (October 2021 to January 2022), summer 2022 (January to April), autumn

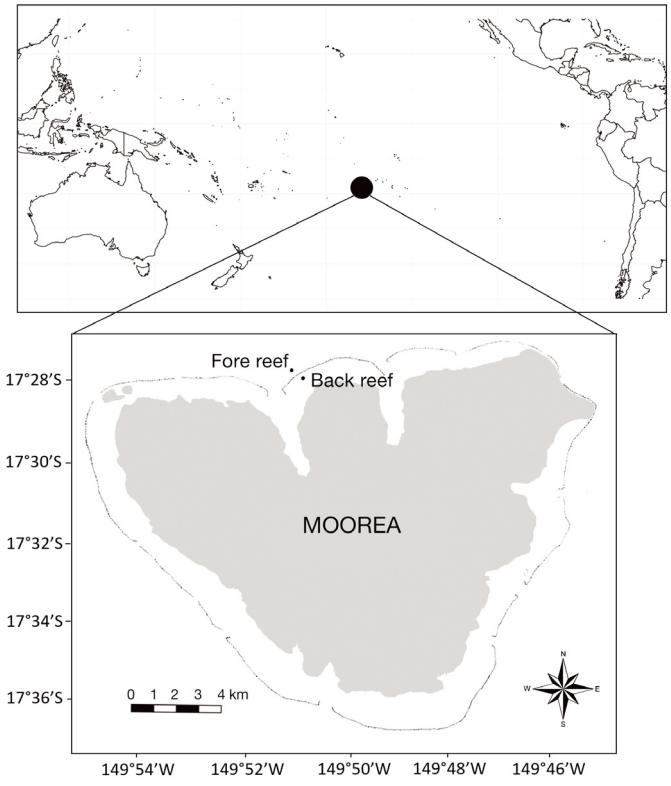

Fig. 1. Moorea Island (French Polynesia), showing the location of the back and fore reef habitats. The line represents the approximate extent of the reef front around Moorea, and the grey sections represent the island of Moorea

2022 (April to June) and winter 2022 (June to October) (Fig. 2; for exact dates, see Table A1 in the Appendix). The seabed on the back reef consisted of scattered massive *Porites* colonies up to 4 m in diameter and 2 m in height, separated by sand and coral rubble. The top of these colonies was mainly colonized by dense canopy-forming macroalgae (mainly *Turbinaria* and *Sargassum*), branching corals, CCA and turf (Bulleri et al. 2022). The fore reef consisted of low-relief coral spur-and-groove formations, primarily covered by branching *Pocillopora* colonies, CCA, turf and low-lying macroalgae (mainly *Lobophora* and *Asparagopsis*); herbivorous fishes were abundant, and nutrients were low (Adam et al. 2022). Despite repeated disturbances over the last decades, the coral communities on the back reef of Moorea have shown remarkable stability, while those on the fore reef have exhibited a relatively consistent recovery (Moritz et al. 2021). Light conditions in each habitat were measured by Dubé et al. (2021), who reported mean and maximum light levels (± SEM) of 446.28 ± 20.99 and 2271.69 ± 63.80 µmol photons m^{-2} s^{-1}, respectively, on the back reef and 137.50 ± 6.82 and 726.38 ± 22.55 µmol photons m^{-2} s^{-1} on the fore reef (13 m). In addition, we recorded temperatures using Onset UA-002-64 HOBO® Pendant temperature loggers placed in unshaded locations at each of the 2 habitats during the entire study duration. The

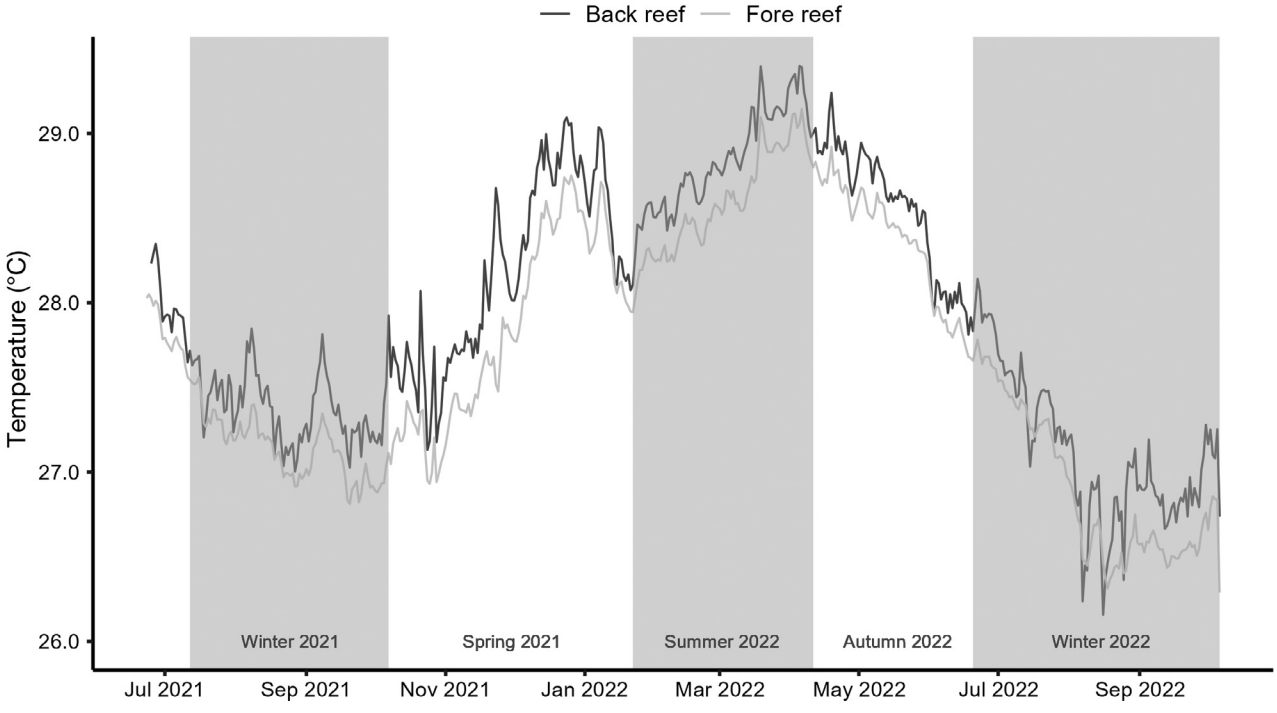

Fig. 2. Daily seawater temperatures at the back reef and fore reef habitats on Moorea from June 2021 to October 2022. Grey and white shading indicates deployment periods

highest daily means occurred at the back reef during the summer 2022 (29.4°C), while the lowest was during the winter 2022 (26.4°C), also at the back reef (Fig. 2). Daily means at the fore reef were on average 0.3°C lower than those at the back reef.

We studied 3 CCA species: *Porolithon onkodes, Neogoniolithon megalocystum* and *Lithophyllum* sp. (Fig. 3). These species were chosen because they (1) are abundant in both reef habitats on the coral reefs of Moorea, (2) can be reliably identified to species level in the field (Jorissen et al. 2020, 2021) and (3) occupy their respective preferred microhabitat within each habitat. We defined exposed microhabitats as small areas within each reef habitat that receive direct sunlight and offer easy access to grazers and good water circulation, and cryptic microhabitats as those not exposed to direct sunlight and less readily accessible to grazers (e.g. holes, overhangs, crevices, cavities), with the subcryptic microhabitats being intermediary (e.g. vertical walls or under overhangs). *P. onkodes* is an important reef builder on coral reefs throughout the tropical Pacific Ocean (Payri et al. 2000, Dean et al. 2015). It typically grows in exposed microhabitats. *N. megalocystum* is found in subcryptic microhabitats, low in light intensity and relatively protected from grazers (Jorissen et al. 2020). Finally, *Lithophyllum* sp. is readily encountered in cryptic microhabitats, such as in coral cavities or on the underside of rubble. CCA samples were identified based on external morphological observations in the field and laboratory (Fig. 3), and DNA analyses were carried out on 24 samples, all species pooled (for exact sample sizes for each species, see Table S1 in the Supplement at www.int-res.com/articles/suppl/m739p031_supp.xlsx). DNA-based identification was conducted on the chloroplast gene *psb*A, the mitochondrial cytochrome c oxidase subunit 1 (COI) gene and 2 rDNAs (small subunit, SSU; and large subunit, LSU). DNA extraction, amplification and sequencing followed Caragnano et al. (2018). The sequences obtained were edited in Geneious version 7.1.9 (www.geneious.com, Kearse et al. 2012). The Basic Local Alignment Search Tool (BLAST; https://blast.ncbi.nlm.nih.gov/, NCBI 1988) was then used to compare our sequences with the GenBank database and assign them to species when possible.

2.2. Sample collection and staining

At the start of each sampling period, we collected 12 fragments of each CCA species using hammer and chisel from each of the 2 reef habitats, at depths of ca. 1–2 m and 12–14 m for the back reef and fore reef, respectively. Each replicate fragment was selected from a haphazardly chosen individual patch. In the laboratory, each specimen was cleaned of epiphytes and cut into a ca. 3 × 2 cm chip with angle pliers. Chips were placed in 5 l of fresh seawater and stained with Alizarin Red Stain at 0.25 g l^{-1} for 18 h. Alizarin is an efficient marker to estimate the growth and calcification of *P. onkodes* at this concentration and immersion time (Lewis & Diaz-Pulido 2017). Treatment containers were kept within a temperature range of 26–28°C under constant aeration. Light intensity was regulated by artificial lights (Aquarium Light System, Viparspectra) above the containers, simulating light-intensity conditions at 12 m depth without any clouds (i.e. 350 µmol quanta m^{-2} s^{-1}) during daylight hours.

After staining, chips were rinsed with fresh seawater to eliminate any residual stain. They were individually embedded within small PVC rings (42 mm diameter × 15 mm height) using epoxy (Minute Mend™) under running seawater, taking care to embed all cut surfaces in the epoxy, and left in flow-through aquaria for 24 h to harden. The purpose of the epoxy ring was to provide a flat surface for surficial marginal growth to occur and to protect the underside skeleton from potential dissolution (Lewis et al. 2017). Two holes were drilled into the lower edge of each PVC ring for later attachment to the reef substratum with cable ties (see below). *P. onkodes* and *N. megalocystum* chips were set with the living crust facing up, while *Lithophyllum* sp. chips were set with the living crust facing down to mimic their respective natural microhabitats (Fig. 4A). Once prepared (ca. 48 h following sample collection), PVC rings with chips were buoyantly weighted using an Ohaus Pioneer PA2102 balance (±0.01 g) for growth and calcification measurements (see Section 2.3). Weight was averaged across 3 repeated measurements. After weighing, samples were photographed in high definition using a Canon EOS6D and a macro 100 mm lens to determine the initial surface area of living CCA tissue (Fig. 4B). Samples were submerged in fresh seawater in a plastic dish placed on a copy stand to ensure the same distance was kept from camera to crust surface throughout the photographs. Two halogen lamps were used to provide even and reproducible illumination. Samples were then returned to the field to the same habitats and depths from which CCA patches were collected. Holes were drilled into dead coral substratum using a pneumatic drill to insert cable tie mounts (Panduit product code HVMPM-08-C0). Each ring was secured to the reef substratum using 2 plastic cable ties, each inserted through the head of 1 cable

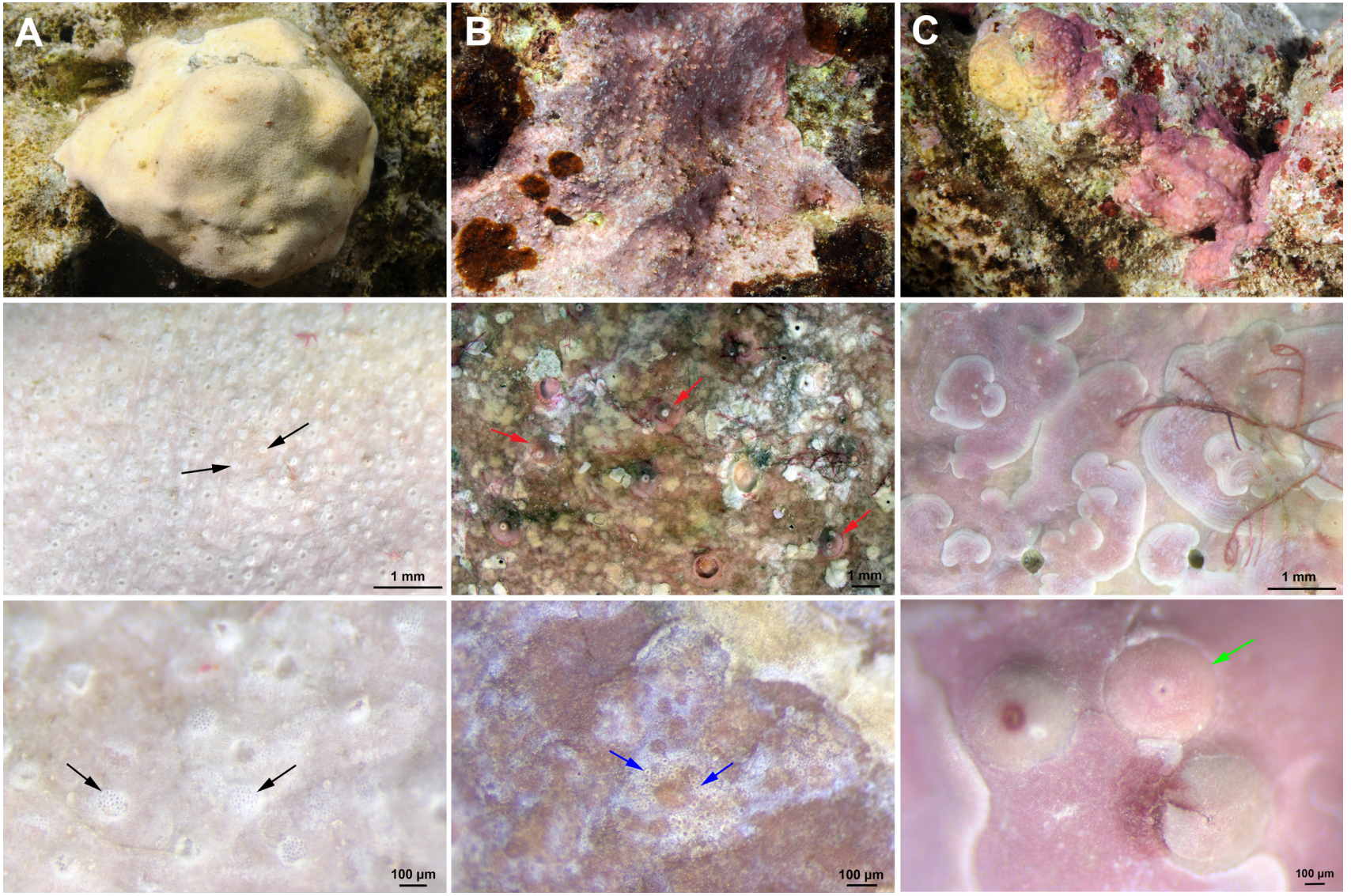

Fig. 3. Field (top row) and microscopic (middle and bottom rows) views of the 3 studied species of crustose coralline algae. (A) *Porolithon* cf. *onkodes*. Note slightly raised fields (black arrows) of densely packed trichocytes homogenously scattered over the crust. (B) *Neogoniolithon* cf. *megalocystum*. Note large (1 mm outside diameter, OD), uniporate conceptacles (red arrows) with a conspicuous tube protruding from the apex and large (15–20 µm OD), white trichocytes (blue arrows) in loose groups irregularly scattered over the crust. (C) *Lithophyllum* sp. Note swirling layers (aplanate branching) with white rims and conical uniporate conceptacles (ca. 600 µm OD, green arrow)

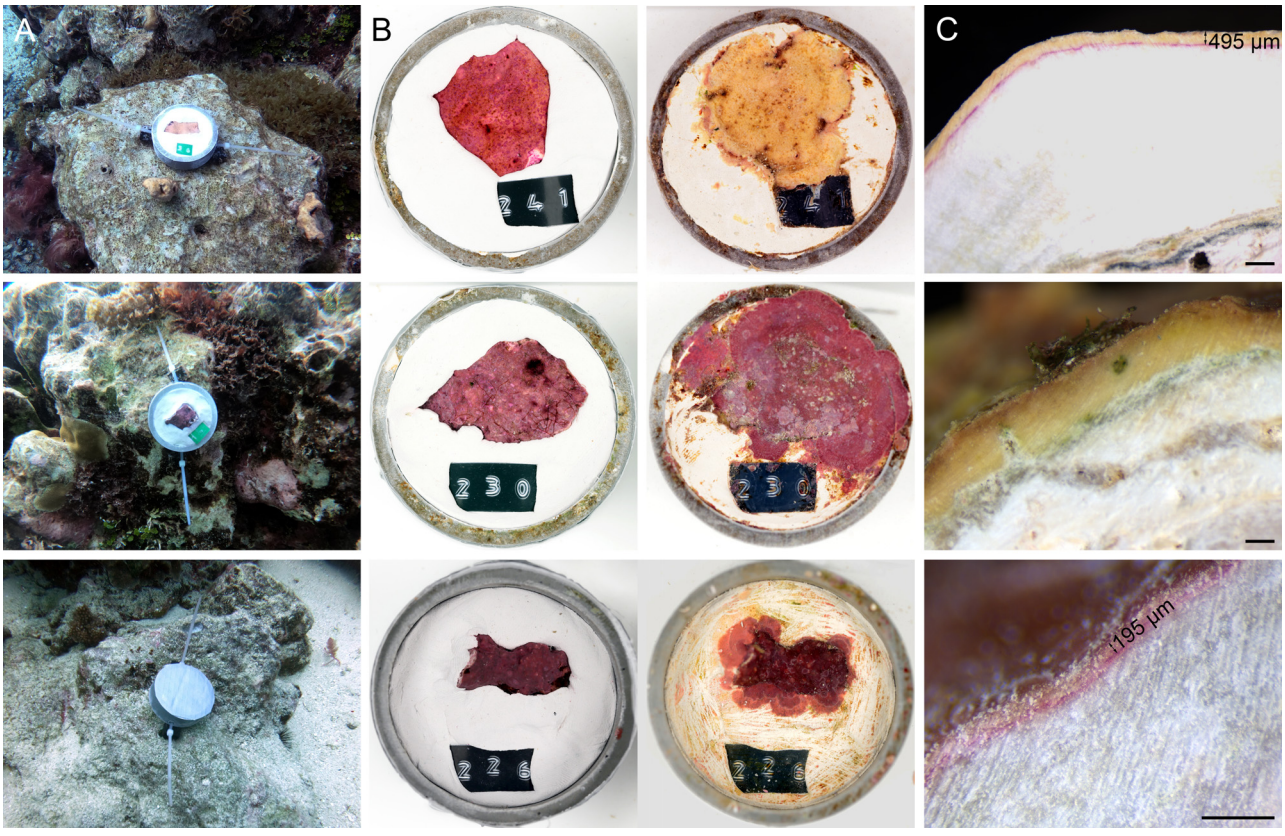

Fig. 4. Top row: *Porolithon* cf. *onkodes*; middle row: *Neogoniolithon* cf. *megalocystum*; bottom row: *Lithophyllum* sp. (A) PVC rings with crustose coralline algae (CCA) chips attached to the reef substratum. Ring diameter = 42 mm. (B) Initial (left) and final (right) photographs of each PVC ring. (C) CCA cross-section cut out at the end of the deployment using a Dremel rotary tool. Lines show measurements of vertical growth from the alizarin stain to the edge of the crust. Scale bars = 500 µm. Note the absence of stain for *N.* cf. *megalocystum*

tie mount and a hole of the PVC ring. This attachment technique resulted in a ca. 10 mm gap between the base of the PCV ring and the reef substratum, allowing for water exchange underneath the ring. CCA species were positioned in their natural microhabitats (i.e. exposed, subcryptic and cryptic for *P. onkodes*, *N. megalocystum* and *Lithophyllum* sp., respectively) as follows: rings with *P. onkodes* chips were placed horizontally with direct exposure to sunlight, rings with *N. megalocystum* chips were placed vertically under overhangs, and rings with *Lithophyllum* sp. were placed horizontally with the CCA facing the reef substratum (Fig. 4A).

Following each deployment period, all samples were collected and replaced with rings with new CCA chips (prepared as described above) for the next period. The same cable tie mounts were used, allowing the rings to be positioned in the exact same places. After careful removal of fouling organisms, PVC rings with chips were buoyantly weighted and photographed (as described above) before being oven-dried at 60°C for 24 h. Samples that showed no extension of the crust over the epoxy were not included in the subsequent measurements to exclude samples which may have been impacted by the experimental procedure (i.e. staining, cutting, setting in epoxy). Only 1 sample was lost during the entire experiment.

2.3. Health, growth and calcification measurements

CCA health variables included rates of partial tissue paling and mortality. Tissue paling was calculated as the percentage of tissue area being discoloured (i.e. pale pink or yellow), but not dead, on the CCA crust (from the final photograph) using ImageJ software. Tissue mortality was calculated as the percentage of dead tissue area. In addition, we recorded the occurrence of epiphytes for each sample when epiphytes were present on the surface or margin of the living crust.

We defined marginal growth as the lateral extension of the living crust. The perimeter and surface area of living crust were derived by tracing around the

edge of the crust in the initial and final photographs using ImageJ software. Marginal growth was computed by dividing the increase in surface area between the initial and final measurements by the initial perimeter of the crust and expressed in mm d^{-1}. The annual marginal growth rate was calculated by summing the average daily growth in each of the 4 seasons (normalised to 91 d $season^{-1}$).

We defined vertical growth as the vertical increase in crust thickness. A ca. 3 mm thick cross section of each oven-dried sample was sliced from the middle of the crust using a Dremel rotary tool with a diamond cut wheel. Vertical growth was obtained by measuring the distance between the alizarin mark and the growing edge of the crust under a compound microscope (Fig. 4C) and expressed in µm d^{-1}. One measure was taken in the middle of the crust along the cross section. As for marginal growth, the annual vertical growth rate was computed by summing the average daily growth in each of the 4 seasons (normalised to 91 d $season^{-1}$).

Net calcification was determined by the buoyant weight method (Jokiel 1978). Weight was converted to dry weight based on the density of skeletal calcium carbonate and seawater following Davies (1989). Net calcification was calculated as the difference between the initial and final weight (W_0 and W_1), normalised to the surface area of living crust (initial and final surface area: A_0 and A_1), and the number of days (d), and expressed in g $CaCO_3$ cm^{-2} yr^{-1}:

$$\text{Net calcification} = \frac{W_1 - W_0}{\left(A_0 + A_1\right)/2}/d \times 365 \quad (1)$$

Annual net calcification was computed by summing the average daily net calcification in each of the 4 seasons (normalised to 91 d $season^{-1}$).

2.4. Statistical analysis

All statistical analyses were performed using R (v.4.2.2). Since the different CCA species varied greatly in their ecology and growth patterns, we analysed the different metrics for each species separately. Prior to analysis, data were tested for normality (Shapiro–Wilk test) and homogeneity of variance (Levene's test) using the 'Shapiro_test' and 'levene_test' functions of the 'rstatix' package. Since tissue paling and mortality data did not meet these assumptions, a 2-way aligned rank transform ANOVA was used to test the differences between habitat (2 levels, fixed) and time period (5 levels, fixed) on these 2 variables using the 'art' function of the 'ARTool' package (Elkin et al. 2021), followed by Tukey's HSD pairwise comparisons using the same package with the 'art.con' function. A multiple logistic regression was run on the presence of epiphytes using the 'glm' function. Tukey pairwise comparisons were performed using the 'glht' function of the 'multcomp' package. A 2-way parametric ANOVA was carried out to test the differences between habitat and time period on marginal and vertical growth and net calcification rates using the 'rstatix' package, followed by Tukey's HSD pairwise comparisons using same package. Unlike net calcification, marginal and vertical growth data did not meet assumptions of normal distribution and homogeneity of variance and were rank-transformed prior to the analysis to meet assumptions of parametric ANOVA. The alizarin staining rarely produced usable marks in *N. megalocystum*, and individuals with usable marks hardly showed any vertical growth, so differences in vertical growth rates were not analysed for this species.

3. RESULTS

3.1. Species identification

A total of 65 sequences was obtained from the samples (i.e. 16 PsbA, 11 COI, 16 SSU and 22 LSU) and submitted to GenBank (under accession numbers PP351864–PP351952) (see Table S1 for detailed results). The BLAST analyses confirmed that DNA sequences of collected *Porolithon onkodes* individuals were genetically close but not similar to the sequences of *P. onkodes* lectotypes (TRH A26-1494). We therefore assigned our specimen to *P.* cf. *onkodes*. Samples of *Neogoniolithon*, previously identified as *N. fosliei* based on field identification (Jorissen et al. 2020), were genetically different from the latter. They were closer to the sequences of *N. megalocystum*, although there is no type sequence for this species. These specimens were therefore assigned to *N.* cf. *megalocystum*. Finally, sequences of samples of *Lithophyllum*, previously identified as *L. prototypum* based on field identification (Jorissen et al. 2021), did not match those of *L. prototypum* from the GenBank database or any other described species. We therefore assigned these samples to *Lithophyllum* sp.

3.2. Health measurements

The percentage of pale tissue of *P.* cf. *onkodes* varied across habitats (aligned rank transform ANOVA,

Table 1. Results of statistical models testing for habitat (Ha) and time period (Tp) differences in each measurement. Tissue discolouration and tissue mortality were analysed by aligned rank transform ANOVA; presence of epiphytes by a multiple logistic regression; and marginal growth, vertical growth and net calcification by 2-way parametric ANOVA. Marginal and vertical growth were rank-transformed prior to the analysis to meet the assumptions of parametric ANOVA. Conclusions are according to Tukey's test. Significant p-values ($p < 0.05$) are in **bold**. Wi: Winter, Au: Autumn, Sp: Spring, Su: Summer; numbers after seasons indicate years (2021 and 2022). Underlines indicate significant difference between time period according to post hoc conclusion

Sources	*Porolithon* cf. *onkodes*				*Neogoniolithon* cf. *megalocystum*				*Lithophyllum* sp.			
	df	F/χ^2	p	Conclusion	df	F/χ^2	p	Conclusion	df	F/χ^2	p	Conclusion
Tissue discolouration												
Ha	1	22.78	**<0.001**	Back reef < Fore reef	1	8.83	**0.004**	Fore reef < Back reef	1	19.11	**<0.001**	Fore reef < Back reef
Tp	4	1.04	0.391		4	2.86	**0.027**	Au22 Wi22 Sp21 Su22 Wi21	4	2.84	**0.030**	Wi22 Sp21 Au22 Wi21 Su 22
Ha × Tp	4	2.28	0.066		4	2.90	0.055		4	3.04	0.063	
Tissue mortality												
Ha	1	0.36	0.552		1	0.53	0.469		1	0.69	0.407	
Tp	4	0.74	0.576		4	2.91	**0.025**	Sp21 Wi21 Su22 Wi22 Au22	4	1.69	0.161	
Ha × Tp	4	0.77	0.547		4	3.05	0.059		4	0.43	0.434	
Presence of epiphytes												
Ha	1	17.48	**<0.001**	Fore reef < Back reef	1	22.75	**<0.001**	Fore reef < Back reef	1	14.57	<0.001	Back reef < Fore reef
Tp	4	13.76	**0.008**	Wi21 Sp21 Su22 Au22 Wi22	4	17.32	**0.002**	Wi21 Sp21 Wi22 Au22 Su22	4	7.98	0.092	
Ha × Tp	4	5.62	0.228		4	8.14	0.089		4	7.08	0.132	
Marginal growth												
Ha	1	8.06	**<0.001**	Back reef < Fore reef	1	69.42	**<0.001**	Back reef < Fore reef	1	0.73	0.390	
Tp	4	28.66	**<0.001**	Wi21 Au22 Sp21 Wi22 Su22	4	4.37	**0.003**	Su22 Au22 Wi21 Sp22 Wi22	4	0.26	0.900	
Ha × Tp	4	2.18	0.076		4	0.11	0.977		4	1.03	0.400	
Residuals	107				99				72			
Vertical growth												
Ha	1	0.57	0.450						1	0.62	0.435	
Tp	4	9.91	**<0.001**	Wi21 Sp21 Au22 Su22 Wi22					4	2.86	**0.029**	Wi22 Wi21 Su22 Au22 Sp21
Ha × Tp	4	1.89	0.120						4	1.56	0.195	
Residuals	107								72			
Net calcification												
Ha	1	1.76	0.188		1	58.06	**<0.001**	Back reef < Fore reef	1	1.18	0.280	
Tp	4	12.40	**<0.001**	Wi21 Sp21 Au22 Su22 Wi22	4	3.55	**0.009**	Su22 Au22 Wi21 Sp22 Wi22	4	0.41	0.800	
Ha × Tp	4	2.10	0.086		4	0.03	0.997		4	0.85	0.500	
Residuals	106				99				72			

F = 22.78, df = 1, p < 0.001, Table 1). It was 11 times higher on the fore reef (mean ± SEM: 0.33 ± 0.16%) than on the back reef (0.03 ± 0.03%) (Tukey's pairwise comparisons p < 0.05, Fig. 5A, Table A2). However, values were extremely low (⩽1% pale tissue) for any given habitat × time period combination. The percentage of pale tissue of *N.* cf. *megalocystum* varied significantly between habitats and time periods (habitat: F = 8.83, df = 1, p = 0.004; time period: F = 2.86, df = 4, p = 0.027). Specifically, it was 5.2 times higher at the back reef (3.98 ± 1.31%) than at the fore reef (0.76 ± 0.29%), and it was 6.6 times higher in winter 2021 (3.92 ± 3.42%) than in autumn 2022 (0.59 ± 0.20%). Likewise, the percentage of pale tissue of *Lithophyllum* sp. varied between habitats and time periods (habitat: F = 19.11, df = 1, p < 0.00; time period: F = 2.84, df = 4, p = 0.030). It was 4.7 times higher at the back reef (4.23 ± 2.07%) than at the fore reef (0.90 ± 0.90%), and it was reduced by 100% in winter 2022 (0.0 ± 0.0%) compared to summer 2022 (5.96 ± 1.44%).

The percentage of dead tissue of *P.* cf. *onkodes* did not vary between time periods or habitats (Table 1) and remained low (2.47 ± 0.81%) (Fig. 5B, Table A2). The percentage of dead tissue of *N.* cf. *megalocystum* varied between time periods (F = 2.91, df = 4, p = 0.025). It was 11.7 times higher in autumn 2022 (4.46 ± 3.98%) than in spring 2021 (0.38 ± 0.18%). No significant time period or habitat difference in the percentage of dead tissue was found for *Lithophyllum* sp. This

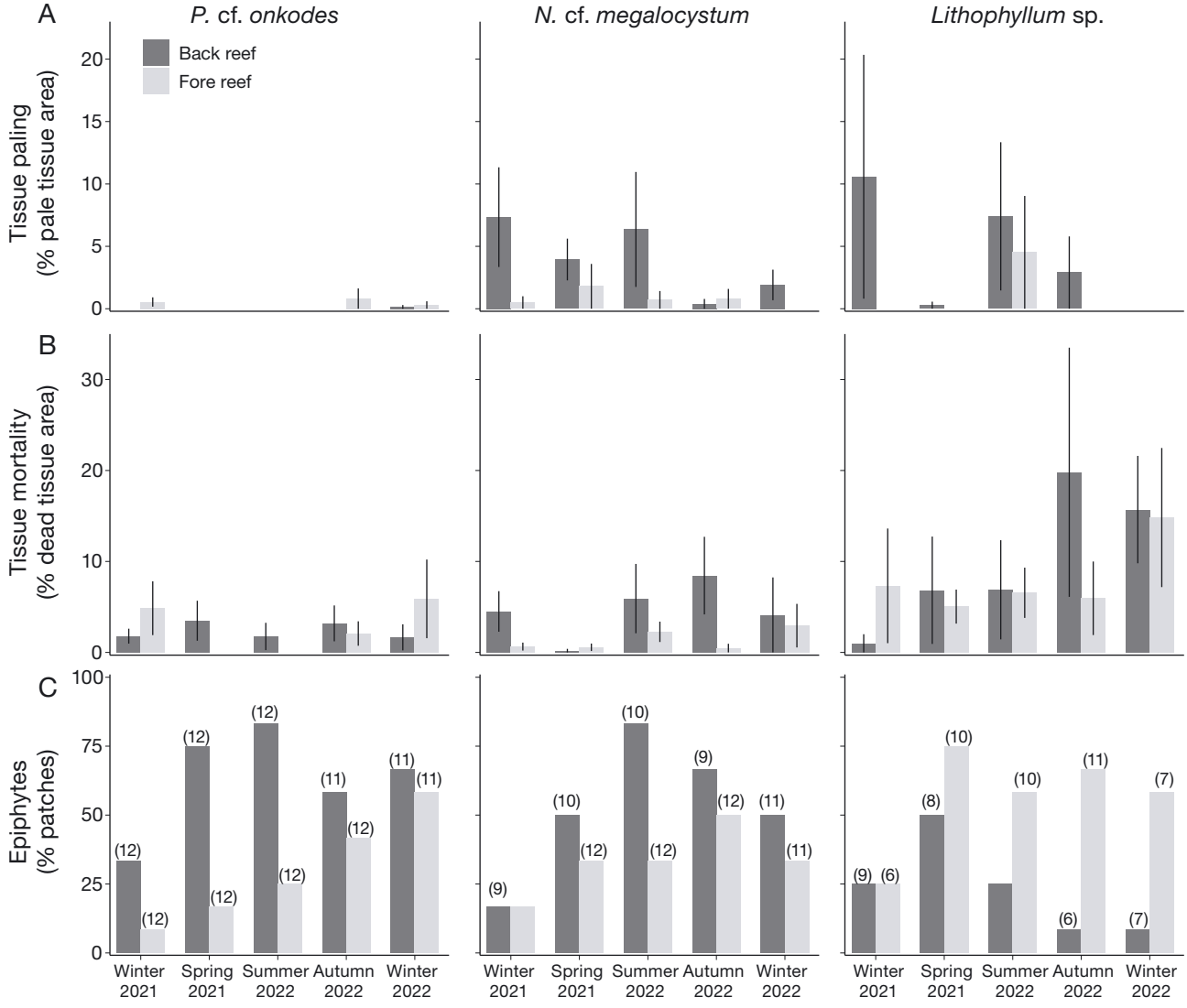

Fig. 5. (A) Partial tissue paling, (B) partial tissue mortality, and (C) percentage of patches with epiphytes of the 3 CCA species at the back reef and fore reef habitats for the different time periods. Data are mean ± SEM. Number of replicates (n) for each factor combination are indicated in (C)

species generally experienced the highest percentage of dead tissue (8.99 ± 2.56%) across all habitat × time period combinations compared to the other 2 taxa.

There were significant effects of habitat and time period on the percentages of *P.* cf. *onkodes* and *N.* cf. *megalocystum* samples with epiphytes (Table 1). The percentage of samples with epiphytes declined from 63.3% at the back reef to 30.0% at the fore reef for *P.* cf. *onkodes*, and from 53.3% at the back reef to 33.3% at the fore reef for *N.* cf. *megalocystum*, representing reductions of 53 and 38% between back reef and fore reef for *P.* cf. *onkodes* and *N.* cf. *megalocystum*, respectively (Fig. 5C). The percentage of *P.* cf. *onkodes* samples with epiphytes was 67% higher in winter 2022 than in winter 2021, while the percentage of *N.* cf. *megalocystum* samples with epiphytes was 71% higher in summer and autumn 2022 than in winter 2021. There was a significant effect of habitat on the percentage of *Lithophyllum* sp. samples with epiphytes (multiple logistic regression, $\chi^2 = 14.57$, df = 1, $p < 0.001$). Unlike the other species, the percentage of *Lithophyllum* sp. samples with epiphytes was reduced by 59% at the back reef compared to that at the fore reef.

3.3. Growth and calcification measurements

There were significant effects of habitat and time period on marginal growth rates of *P.* cf. *onkodes* (2-way parametric ANOVA, habitat: $F_{1,107} = 8.06$, $p < 0.001$; time period: $F_{4,107} = 28.66$, $p < 0.001$; Table 1). Marginal growth of *P.* cf. *onkodes* was 1.8 times higher at the fore reef (0.043 ± 0.003 mm d^{-1}) than at the back reef (0.023 ± 0.002 mm d^{-1}) and was 2.8 times higher in summer 2022 (0.046 ± 0.005 mm d^{-1}) than in winter 2021 (0.016 ± 0.003 mm d^{-1}) (Tukey's pairwise comparisons $p < 0.05$; Fig. 6A, Table A2). There were also significant effects of habitat and time period on marginal growth rates of *N.* cf. *megalocystum* (habitat: $F_{1,99} = 69.42$, $p < 0.001$; time period: $F_{4,99} = 4.37$, $p = 0.003$). Marginal growth of *N.* cf. *megalocystum* was 5.3 times higher at the fore reef (0.043 ± 0.004 mm d^{-1}) than at the back reef (0.008 ± 0.002 mm d^{-1}) and was 3.1 times higher in winter 2022 (0.05 ± 0.01 mm d^{-1}) than in autumn and summer 2022 (0.016 ± 0.004 mm d^{-1}). No significant difference was found in the marginal growth of *Lithophyllum* sp. between habitats or time periods. Seasonal averages for each species × habitat combination gave a minimum annual marginal growth rate of 2.17 mm yr^{-1} for *Lithophyllum* sp. at the back reef and a maximal rate of 15.19 mm yr^{-1} for *P.* cf. *onkodes* at the fore reef (Table 2).

The staining procedure produced visible alizarin marks in all *P.* cf. *onkodes* and *Lithophyllum* sp. samples. However, only 3 out of 108 samples of *N.* cf. *megalocystum* had a distinguishable mark. These produced a vertical growth rate of 0.10 ± 0.09 μm d^{-1}, suggesting that *N.* cf. *megalocystum* shows little to no vertical growth. Thus, vertical growth data were not analysed for this species. Vertical growth varied significantly among time periods for *P.* cf. *onkodes* (2-way parametric ANOVA, $F_{4,107} = 9.91$, $p < 0.001$; Table 1). Values ranged from 3.61 ± 0.25 μm d^{-1} in winter 2021 to 5.69 ± 0.33 μm d^{-1} in winter 2022 (Fig. 6B, Table A2). Post hoc Tukey multiple comparison tests showed that 3 groups of time periods formed homogeneous sets (winter and spring 2021; spring 2021, autumn and summer 2022; autumn, summer and winter 2022). There was a significant effect of time period on vertical growth rates of *Lithophyllum* sp. ($F_{4,72} = 2.86$, $p = 0.029$). Vertical growth of *Lithophyllum* sp. was 3.7 times higher in spring 2021 (1.73 ± 0.34 μm d^{-1}) than in winter 2022 (0.47 ± 0.27 μm d^{-1}). Seasonal averages for each species × habitat combination (excluding *N.* cf. *megalocystum*) gave a minimum annual vertical growth rate of 0.32 mm yr^{-1} for *Lithophyllum* sp. at the fore reef and a maximal rate of 1.55 mm yr^{-1} for *P.* cf. *onkodes* at the fore reef (Table 2).

As with marginal and vertical growth, net calcification of *P.* cf. *onkodes* varied among time periods (2-way parametric ANOVA, $F_{4,106} = 12.40$, $p < 0.001$; Table 1). Values ranged from 0.40 ± 0.03 g $CaCO_3$ cm^{-2} yr^{-1} in winter 2021 to 0.76 ± 0.05 g $CaCO_3$ cm^{-2} yr^{-1} in winter 2022 (Fig. 6C, Table A2). Post hoc Tukey multiple comparison tests showed that 4 groups of time periods formed homogeneous sets (winter and spring 2021; spring 2021 and autumn 2022; autumn and summer 2022; summer and winter 2022). There were significant differences in net calcification of *N.* cf. *megalocystum* across both habitats and time periods (habitat: $F_{1,99} = 58.06$, $p < 0.001$; time period: $F_{4,99} = 3.55$, $p = 0.009$). Net calcification of *N.* cf. *megalocystum* was 4.1 times higher at the fore reef (0.33 ± 0.02 g $CaCO_3$ cm^{-2} yr^{-1}) than at the back reef (0.08 ± 0.03 g $CaCO_3$ cm^{-2} yr^{-1}) and was 2.3 times higher in winter 2022 (0.30 ± 0.05 g $CaCO_3$ cm^{-2} yr^{-1}) than in summer 2022 (0.13 ± 0.04 g $CaCO_3$ cm^{-2} yr^{-1}). Net calcification of *Lithophyllum* sp. showed no difference across habitats or time periods. Seasonal averages for each species × habitat combination gave a minimum annual net calcification rate of 0.02 g $CaCO_3$ cm^{-2} yr^{-1} for *Lithophyllum* sp. at the back reef and a maximal rate of 0.55 g $CaCO_3$ cm^{-2} yr^{-1} for *P.* cf. *onkodes* at the fore reef (Table 2).

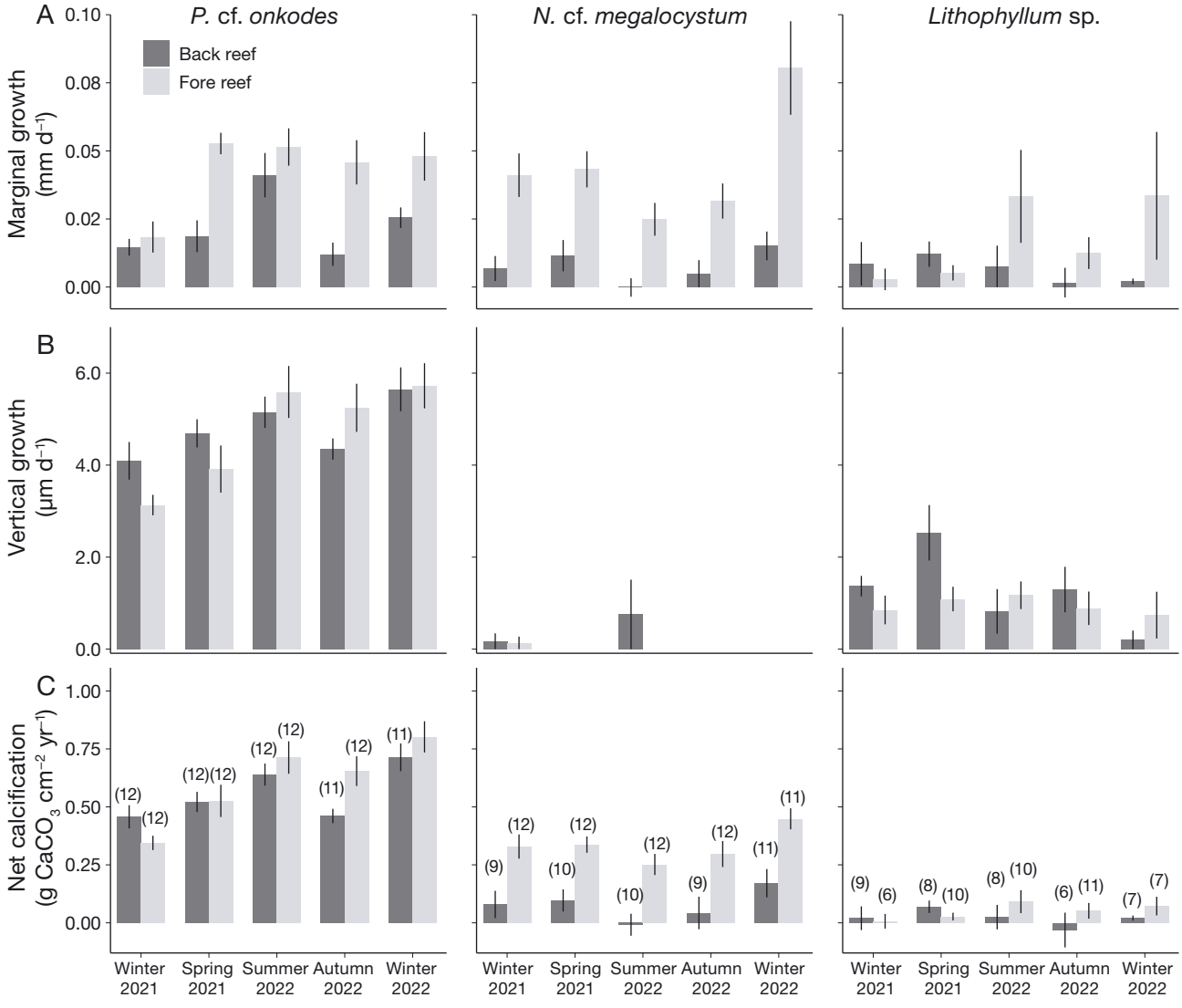

Fig. 6. (A) Marginal growth, (B) vertical growth, and (C) net calcification rates of the 3 CCA species at the back reef and fore reef habitats for the different time periods. Data are mean ± SEM. Number of replicates (n) for each factor combination are indicated in (C)

4. DISCUSSION

Our results validate our first hypothesis that CCA growth and calcification rates are highest in the exposed species, intermediate in the subcryptic species and lowest in the cryptic species. Annual net calcification rates averaged across habitats were highest in exposed *Porolithon* cf. *onkodes* (0.51 g $CaCO_3$ cm^{-2} yr^{-1}), intermediate in subcryptic *Neogoniolithon* cf. *megalocystum* (0.16 g $CaCO_3$ cm^{-2} yr^{-1}) and lowest in cryptic *Lithophyllum* sp. (0.03 g $CaCO_3$ cm^{-2} yr^{-1}). Similar trends were observed for annual marginal growth rates. The microhabitat greatly affects net calcification rates by CCA (Adey & Vassar 1975) and encrusting communities (Mallela 2007, Morgan & Kench 2017). Cryptic CCA species may be adapted to low-light environments and benefit from lower herbivory pressure and algal biomass in their habitat (Chisholm 2000). However, their calcification may be limited due to reduced light availability (i.e. limiting carbohydrate production from photosynthesis required for growth and calcification, Payri et al. 2001) and water motion (i.e. which regulates nutrient and gas exchanges, Leigh et al. 1987). For example, CCA crusts in areas of low hydrodynamic energy are more porous (Martindale 1992, Gherardi & Bosence 2001).

CCA are notoriously difficult to identify in the field (Caragnano et al. 2018, Gabrielson et al. 2018), and

Table 2. Annual marginal and vertical growth and net calcification rates of the 3 crustose coralline algae species in the back reef and fore reef habitats

	P. cf. *onkodes*	*N.* cf. *megalocystum*	*Lithophyllum* sp.
Marginal growth (mm yr^{-1})			
Back reef	7.46	2.22	2.17
Fore reef	15.19	11.89	5.50
Pooled habitats	11.32	7.05	3.84
Vertical growth (mm yr^{-1})			
Back reef	1.52	0.07	0.46
Fore reef	1.55	0.01	0.32
Pooled habitats	1.53	0.04	0.39
Net calcification (g $CaCO_3$ cm^{-2} yr^{-1})			
Back reef	0.48	0.06	0.02
Fore reef	0.55	0.27	0.05
Pooled habitats	0.51	0.16	0.03

few studies to date have taken all the relevant steps for their identification. In the present study, identification based on external morphological observations in the field and laboratory for all 3 species matched well with their DNA-based identification. Although this may not work for all species, these results support that future studies should couple detailed morphological observations with genetic characterisation, at least on a subset of samples.

Marginal growth rates (0.3–1.65 mm mo^{-1}) of *P.* cf. *onkodes* were within the range of those found by other studies for this species (e.g. 1.53–2.52 mm mo^{-1} in Lewis et al. 2017 and Table 3 therein for earlier records), as well as a recent study on the fore reef of Moorea (1.21 mm mo^{-1}, Jorissen et al. 2020). Similarly, annual vertical growth rates (1.5 mm yr^{-1}) of *P.* cf. *onkodes* were within the expected range for this species based on previous studies (e.g. 1.4 mm yr^{-1} in Lewis et al. 2017 and Table 3 therein). Its annual net calcification averaged 0.48 and 0.55 g $CaCO_3$ cm^{-2} yr^{-1} at the back reef and fore reef habitats, respectively. These values are of the same order of magnitude as those published for this species by Payri (1995, 1997) in Moorea (0.41 g $CaCO_3$ cm^{-2} yr^{-1}) or by Chisholm et al. (1990) on the reef crest at Lizard Island in the Great Barrier Reef (0.31 g $CaCO_3$ cm^{-2} yr^{-1}). They are lower than those found by Lewis et al. (2017) for this species on the outer slope of Heron Island in the Great Barrier Reef (2.72–3.40 g $CaCO_3$ cm^{-2} yr^{-1}), but higher than those found by Goh et al. (2021) for encrusting organisms dominated by CCA in turbid reefs off Singapore (0.009 to 0.052 g $CaCO_3$ cm^{-2} yr^{-1}). Differences between studies may be related to differences in methods, environmental conditions and/or seasons. *P. onkodes* is well adapted to high-light environments (Tâmega & Figueiredo 2019) and typically dominates shallow and sunlit reefs (Payri 2000). Together with its widespread distribution throughout the tropical Pacific Ocean (Payri et al. 2000, Dean et al. 2015), our data confirm the importance of *P. onkodes* in reef carbonate production.

Annual net calcification rates of *N.* cf. *megalocystum* and *Lithophyllum* sp. approached those reported for cryptic encrusting communities (i.e. 0.066 g $CaCO_3$ cm^{-2} yr^{-1}, Morgan & Kench 2017). While the annual net calcification rates of *Lithophyllum* sp. were on average 17 times lower than those of *P* cf. *onkodes*, it should be noted that cryptic surfaces can account for up to 82% of the total reef surface area and that calcifying algae occupy approximately 15 and 35% of the exposed and cryptic surfaces, respectively (Kornder et al. 2021). Together, these data underline the need to include calcification by subcryptic and cryptic CCA species in reef carbonate budgets. *Lithophyllum* sp. had low net calcification rates associated with low marginal and vertical growth rates. In addition, this species showed the highest rates of partial tissue paling (~4 and ~1% for the back reef and fore reef, respectively, averaged across time intervals) and mortality (~9% averaged across habitats and time intervals). Exposure to very low light levels can cause tissue discolouration and partial mortality in CCA (Bessell-Browne et al. 2017). As a cryptic species, *Lithophyllum* sp. is likely to be well adapted to low light levels. However, this species forms a thin crust with a single-layer hypothallium and a perithallium that consists of a single layer or is absent. This growth form is often heavily grazed and outcompeted (Adey & Vassar 1975, Arnold & Steneck 2011, McCoy & Pfister 2014). In contrast, *P. onkodes* and *N. megacystum* have well developed thick crusts which are more resilient to damage and quickly regenerate (Steneck 1986, Steneck et al. 1991).

Our alizarin staining protocol resulted in visible marks in both *P.* cf. *onkodes* and *Lithophyllum* sp., but not in *N.* cf. *megalocystum*, which showed little to no vertical growth. Alizarin produces greater mark visibility on CCA individuals that have high growth rates (Lewis & Diaz-Pulido 2017). While alizarin has been widely used to stain several CCA species without affecting growth (Andrake & Johansen 1980, Blake & Maggs 2003, Steller et al. 2007), the toxicity of alizarin can potentially reduce CCA and coral calcification rates for several days immediately following staining (Dodge et al. 1984, Payri 1997). Since we used a concentration and immersion time which have been demonstrated to be not toxic to *P. onkodes* (Lewis & Diaz-

Pulido 2017), we are confident that our results are representative at least for this species. Marginal growth rates (0.77–2.49 mm mo^{-1}) of *N.* cf. *megalocystum* were lower than those of unstained individuals reported on the fore reef of Moorea (2.89 mm mo^{-1}, Jorissen et al. 2020), which could suggest an inhibitory effect. It would have been useful to compare our marginal growth and calcification rates with those of non-stained individuals to evaluate potential alizarin effects, but this was out of the scope of the present study.

Our results demonstrate significant differences among time periods in all measured growth and calcification variables. However, they do not support a strong seasonal pattern in growth and calcification rates of CCA in Moorea. We can reject our second hypothesis that maximum seasonal growth and calcification rates occur over the summer season. While marginal growth and calcification rates of *P.* cf. *onkodes* were higher in summer 2022 than in winter 2021, differences between summer 2022 and winter 2022 were not significant. Likewise, there were no consistent seasonal trends for *N.* cf. *megalocystum* and *Lithophyllum* sp. Although marginal growth and calcification rates of *N.* cf. *megalocystum* were lower in summer 2022 than in winter 2022, differences between summer 2022 and winter 2021 were not significant. This lack of summer maxima contrasts with the study of Payri (1997) showing higher calcification rates of the rhodolith *Hydrolithon reinboldii* in the summer in Moorea, as well as previous studies from tropical (Pulecio-Plaza et al. 2023), temperate (Adey & McKibbin 1970, Martin et al. 2006, Kamenos & Law 2010, Burdett et al. 2011, Egilsdottir et al. 2016) and polar (Adey 1970, Blake & Maggs 2003, Halfar et al. 2008) regions. However, it agrees with the studies of Short et al. (2015) and Lewis et al. (2017). On the Great Barrier Reef, maximum seasonal growth and calcification rates of *P. onkodes* did not occur over the summer (Lewis et al. 2017). Deviations in expected summer maxima may be explained by elevated temperature, low seasonal temperature variability and various stress factors during the summer season (Lewis et al. 2017). Short et al. (2015) found a distinct lack of seasonality in temperate CCA species belonging to the sub-family Hydrolithoideae following a marine heatwave off Western Australia. In our study, water temperatures were typical, with summer maxima not surpassing the coral bleaching threshold reported for Moorea (i.e. 29.2°C; Adjeroud et al. 2002). Daily mean temperature varied by only 3°C between winter and summer, which is less than that of the Great Barrier Reef reported by Lewis et al. (2017) (i.e. 5°C) or of the Artic region (i.e. 12°C, Freiwald & Henrich 1994), making it the most likely explanatory factor.

We found significant spatial differences in the marginal growth rates of *P.* cf. *onkodes* and *N.* cf. *megalocystum*. For both species, marginal growth rates were higher at the fore reef compared to the back reef. In addition, *N.* cf. *megalocystum* also showed higher rates of net calcification at the fore reef. These differences could be explained by a combination of increased herbivory and decreased light levels at the fore reef, which may have resulted in less vigorous epiphytic growth. In our study, this hypothesis is supported by the lower occurrence of epiphytes on both *P.* cf. *onkodes* and *N.* cf. *megalocystum* at the fore reef. The fore reefs of Moorea typically exhibit higher herbivory and lower light levels relative to the back reefs (Adam et al. 2011, 2022, Dubé et al. 2021). CCA need herbivores to remove epiphytes, especially turf algae, which limit their growth by trapping sediments (Steneck 1986, Williams & Carpenter 1990, Steneck 1997, Figueiredo et al. 2000). CCA are typically more abundant in shallow environments, where herbivore pressure and wave exposure reduce turf algal biomass, as well as in deeper or cryptic habitats, where light intensities are not sufficient to sustain the fast growth of competitive species (Chisholm 2000). In the Abrolhos, the lateral growth of *P. onkodes* is positive on the reef edge and base, but zero on the reef flat, which is explained by desiccation and high epiphytic cover of non-calcareous crusts due to low herbivory (Figueiredo & Steneck 2002, Tâmega et al. 2016). In addition, CCA species show various degrees of photoinhibition depending on light exposure during growth (Payri et al. 2001). For example, shaded fragments of *P. onkodes* grow faster (both vertically and marginally) than those in full sunlight on the Great Barrier Reef (Lewis et al. 2017). Photoinhibition may be more pronounced in shaded plants (Payri et al. 2001), which is consistent with the large differences in both growth and calcification of *N.* cf. *megalocystum* between the fore reef and back reef. Furthermore, the relatively low growth and calcification rates of this species in the summer period at both habitats suggests that photoinhibition could be exacerbated by elevated water temperature, which is consistent with other studies (e.g. Vásquez-Elizondo & Enríquez 2016).

This study increases our knowledge on the growth and calcification of CCA in the South Pacific. Our results reveal that CCA growth and calcification is species-specific and can be spatially and temporally variable. They support the need to consider spatio-temporal variations in calcification rates, as well as

calcification by subcryptic and cryptic species, to improve the accuracy of reef carbonate budgets. Field census-based assessment of CCA cover and species composition residing in subcryptic and cryptic microhabitats is clearly challenging, but quantifying benthic communities in these microhabitats has been successfully conducted using endoscopic and 3D reconstruction approaches (Richter et al. 2001, Korndер et al. 2021). In addition, sampling in the field should be coupled with external morphological observations and molecular identification to increase our understanding of the contribution of different species to calcification. Similar studies should be conducted at other locations to explore inter-annual and inter-habitat variabilities in coralline algal growth and calcification. *In situ* studies such as this one provide important baseline information to understand how CCA communities are responding to environmental changes.

Data accessibility. Raw data can be downloaded from a Zenodo repository with restricted access: https://zenodo.org/records/11151720.

Acknowledgements. We thank Pierre-Louis Rault, Hugo Bischoff and Axel Urbanowiez for their help in the field. We also thank Fabien Morat for his assistance in data measurements and the staff of the CRIOBE research station. Molecular analyses were performed at the Plateforme du Vivant (CRESICA-IRD Noumea). The present work was part of C.V.'s PhD thesis. This work was supported by the French National Research Agency through the project CORALMATES (ANR-18-CE02-0009-01).

LITERATURE CITED

Adam TC, Schmitt RJ, Holbrook SJ, Brooks AJ, Edmunds PJ, Carpenter RC, Bernardi G (2011) Herbivory, connectivity, and ecosystem resilience: response of a coral reef to a large-scale perturbation. PLOS ONE 6:e23717

Adam TC, Holbrook SJ, Burkepile DE, Speare KE and others (2022) Priority effects in coral–macroalgae interactions can drive alternate community paths in the absence of top-down control. Ecology 103:e3831

Adey WH (1970) The effects of light and temperature on growth rates in boreal-subartic crustose corallines. J Phycol 6:269–276

Adey WH (1978) Algal ridges of the Caribbean sea and West Indies. Phycologia 17:361–367

Adey WH, McKibbin DL (1970) Studies on the maerl species *Phymatolithon calcareum* (Pallas) nov. comb. and *Lithothamnium coralloides* Crouan in the Ria de Vigo. Bot Mar XIII:100–106

Adey WH, Vassar JM (1975) Colonization, succession and growth rates of tropical crustose coralline algae (Rhodophyta, Cryptonemiales). Phycologia 14:55–69

Adjeroud M, Augustin D, Galzin R, Salvat B (2002) Natural disturbances and interannual variability of coral reef communities on the outer slope of Tiahura (Moorea, French Polynesia): 1991 to 1997. Mar Ecol Prog Ser 237:121–131

Andrake W, Johansen HW (1980) Alizarin red dye as a marker for measuring growth in *Corallina officinalis* L. (Corallinaeae, Rhodophyta). J Phycol 16:620–622

Arnold SN, Steneck RS (2011) Settling into an increasingly hostile world: the rapidly closing 'recruitment window' for corals. PLOS ONE 6:e28681

Bak RPM (1976) The growth of coral colonies and the importance of crustose coralline algae and burrowing sponges in relation with carbonate accumulation. Neth J Sea Res 10:285–337

Bessell-Browne P, Negri AP, Fisher R, Clode PL, Jones R (2017) Impacts of light limitation on corals and crustose coralline algae. Sci Rep 7:11553

Birrell CL, McCook LJ, Willis BL, Harrington L (2008) Chemical effects of macroalgae on larval settlement of the broadcast spawning coral *Acropora millepora.* Mar Ecol Prog Ser 362:129–137

Blake C, Maggs CA (2003) Comparative growth rates and internal banding periodicity of maerl species (Corallinales, Rhodophyta) from northern Europe. Phycologia 42:606–612

Browne NK, Cuttler M, Moon K, Morgan K and others (2021) Predicting responses of geo-ecological carbonate reef systems to climate change: a conceptual model and review. Oceanogr Mar Biol Annu Rev 59:229–370

Bulleri F, Pozas-Schacre C, Bischoff H, Bramanti L, D'agata S, Gasc J, Nugues MM (2022) Compounded effects of sea urchin grazing and physical disturbance on macroalgal canopies in the lagoon of Moorea, French Polynesia. Mar Ecol Prog Ser 697:45–56

Burdett H, Kamenos NA, Law A (2011) Using coralline algae to understand historic marine cloud cover. Palaeogeogr Palaeoclimatol Palaeoecol 302:65–70

Caragnano A, Foetisch A, Maneveldt GW, Millet L and others (2018) Revision of Corallinaceae (Corallinales, Rhodophyta): recognizing *Dawsoniolithon* gen. nov., *Parvicellularium* gen. nov. and Chamberlainoideae subfam. nov. containing *Chamberlainium* gen. nov. and *Pneophyllum.* J Phycol 54:391–409

Chisholm JRM (2000) Calcification by crustose coralline algae on the northern Great Barrier Reef, Australia. Limnol Oceanogr 45:1476–1484

Chisholm JRM, Collingwood JC, Gill EF (1990) A novel in situ respirometer for investigating photosynthesis and calcification in crustose coralline algae. J Exp Mar Biol Ecol 141:15–29

Cornwall CE, Carlot J, Branson O, Courtney TA and others (2023) Crustose coralline algae can contribute more than corals to coral reef carbonate production. Commun Earth Environ 4:105

Courtney TA, De Carlo EH, Page HN, Bahr KD and others (2018) Recovery of reef-scale calcification following a bleaching event in Kāne'ohe Bay, Hawai'i. Limnol Oceanogr Lett 3:1–9

Courtney TA, Barkley HC, Chan S, Courtney CS and others (2022) Rapid assessments of Pacific Ocean net coral reef carbonate budgets and net calcification following the 2014–2017 global coral bleaching event. Limnol Oceanogr 67:1687–1700

Davies PS (1989) Short-term growth measurements of corals using an accurate buoyant weighing technique. Mar Biol 101:389–395

Dean AJ, Steneck RS, Tager D, Pandolfi JM (2015) Distribu-

tion, abundance and diversity of crustose coralline algae on the Great Barrier Reef. Coral Reefs 34:581–594
Deinhart M, Mills MS, Schils T (2022) Community assessment of crustose calcifying red algae as coral recruitment substrates. PLOS ONE 17:e0271438
Diaz-Pulido G, Anthony KRN, Kline DI, Dove S, Hoegh-Guldberg O (2012) Interactions between ocean acidification and warming on the mortality and dissolution of coralline algae. J Phycol 48:32–39
Dodge RE, Wyers SC, Frith HR, Knap AH, Smith SR, Cook CB, Sleeter TD (1984) Coral calcification rates by the buoyant weight technique: effects of alizarin staining. J Exp Mar Biol Ecol 75:217–232
Dubé CE, Ziegler M, Mercière A, Boissin E, Planes S, Bourmaud CAF, Voolstra CR (2021) Naturally occurring fire coral clones demonstrate a genetic and environmental basis of microbiome composition. Nat Commun 12:6402
Egilsdottir H, Olafsson J, Martin S (2016) Photosynthesis and calcification in the articulated coralline alga *Ellisolandia elongata* (Corallinales, Rhodophyta) from intertidal rock pools. Eur J Phycol 51:59–70
Elkin LA, Kay M, Higgins JJ, Wobbrock JO (2021) An aligned rank transform procedure for multifactor contrast tests. In: Nichols J, Kumar R, Nebeling M (eds) Proceedings of UIST '21: The 34th Annual ACM Symposium on User Interface Software and Technology. October 10–14, 2021, Virtual Event, USA. Association for Computing Machinery, New York, NY, p 754–768
Fabricius K, De'ath G (2001) Environmental factors associated with the spatial distribution of crustose coralline algae on the Great Barrier Reef. Coral Reefs 19:303–309
Figueiredo MAO (1997) Colonization and growth of crustose coralline algae in Abrolhos, Brazil. Proc 8th Int Coral Reef Symp 1:689–694
Figueiredo MAO, Kain (Jones) JM, Norton TA (2000) Responses of crustose corallines to epiphyte and canopy cover. J Phycol 36:17–24
Figueiredo MAO, Steneck RS (2002) Floristic and ecological studies of crustose coralline algae on Brazil's Abrolhos reefs. Proc 9th Int Coral Reef Symp 1:493–498
Freiwald A, Henrich R (1994) Reefal coralline algal build-ups within the Arctic Circle: morphology and sedimentary dynamics under extreme environmental seasonality. Sedimentology 41:963–984
Gabrielson PW, Hughey JR, Diaz-Pulido G (2018) Genomics reveals abundant speciation in the coral reef building alga *Porolithon onkodes* (Corallinales, Rhodophyta). J Phycol 54:429–434
Gherardi DFM, Bosence DWJ (2001) Composition and community structure of the coralline algal reefs from Atol das Rocas, South Atlantic, Brazil. Coral Reefs 19:205–219
Gherardi DFM, Bosence DWJ (2005) Late Holocene reef growth and relative sea-level changes in Atol das Rocas, equatorial South Atlantic. Coral Reefs 24:264–272
Goh TZY, Bauman AG, Januchowski-Hartley FA, Morgan KM, Seah JCL, Todd PA (2021) Growth and carbonate production of crustose coralline algae on a degraded turbid reef system. Mar Pollut Bull 173:113135
Gómez-Lemos LA, Diaz-Pulido G (2017) Crustose coralline algae and associated microbial biofilms deter seaweed settlement on coral reefs. Coral Reefs 36:453–462
Gómez-Lemos LA, Doropoulos C, Bayraktarov E, Diaz-Pulido G (2018) Coralline algal metabolites induce settlement and mediate the inductive effect of epiphytic microbes on coral larvae. Sci Rep 8:17557
Halfar J, Steneck R, Schöne B, Moore GWK and others (2008) Coralline alga reveals first marine record of subarctic North Pacific climate change. Geophys Res Lett 34:L07702
Harrington L, Fabricius K, De'ath G, Negri A (2004) Recognition and selection of settlement substrata determine post-settlement survival in corals. Ecology 85:3428–3437
Heyward AJ, Negri AP (1999) Natural inducers for coral larval metamorphosis. Coral Reefs 18:273–279
Ichiki S, Mizuta H, Yasui H, Yamamoto H (2001) Effects of irradiance and water temperature on the photosynthesis and growth of the crustose coralline alga *Lithophyllum yessoense* Foslie (Corallinales, Rhodophyceae). Bull Fac Fish Hokkaido Univ 52:103–109
Jokiel P (1978) Coral growth: buoyant weight technique. In: Stoddart DR, Johannes RE (eds) Coral reefs: research methods. UNESCO, Paris, p 529–541
Jorissen H, Baumgartner C, Steneck RS, Nugues MM (2020) Contrasting effects of crustose coralline algae from exposed and subcryptic habitats on coral recruits. Coral Reefs 39:1767–1778
Jorissen H, Galand PE, Bonnard I, Meiling S and others (2021) Coral larval settlement preferences linked to crustose coralline algae with distinct chemical and microbial signatures. Sci Rep 11:14610
Kamenos NA, Law A (2010) Temperature controls on coralline algal skeletal growth. J Phycol 46:331–335
Kearse M, Moir R, Wilson A, Stones-Havas S and others (2012) Geneious Basic: an integrated and extendable desktop software platform for the organization and analysis of sequence data. Bioinformatics 28:1647–1649
Kendrick GA (1991) Recruitment of coralline crusts and filamentous turf algae in the Galapagos archipelago: effect of simulated scour, erosion and accretion. J Exp Mar Biol Ecol 147:47–63
Kornder NA, Cappelletto J, Mueller B, Zalm MJL and others (2021) Implications of 2D versus 3D surveys to measure the abundance and composition of benthic coral reef communities. Coral Reefs 40:1137–1153
Kuffner IB, Andersson AJ, Jokiel PL, Rodgers KS, Mackenzie FT (2008) Decreased abundance of crustose coralline algae due to ocean acidification. Nat Geosci 1:114–117
Leigh EG, Paine RT, Quinn JF, Suchanek TH (1987) Wave energy and intertidal productivity. Proc Natl Acad Sci USA 84:1314–1318
Lewis B, Diaz-Pulido G (2017) Suitability of three fluorochrome markers for obtaining *in situ* growth rates of coralline algae. J Exp Mar Biol Ecol 490:64–73
Lewis B, Kennedy EV, Diaz-Pulido G (2017) Seasonal growth and calcification of a reef-building crustose coralline alga on the Great Barrier Reef. Mar Ecol Prog Ser 568:73–86
Littler MM (1973) The population and community structure of Hawaiian fringing-reef crustose Corallinaceae (Rhodophyta, Cryptonemiales). J Exp Mar Biol Ecol 11:103–120
MacIntyre IG (1997) Re-evaluating the role of crustose algae in the construction of coral reefs. Proc 8th Int Coral Reef Symp 1:725–730
Mallela J (2007) Coral reef encruster communities and carbonate production in cryptic and exposed coral reef habitats along a gradient of terrestrial disturbance. Coral Reefs 26:775–785
Mallela J (2013) Calcification by reef-building sclerobionts. PLOS ONE 8:e60010
Martin S, Gattuso JP (2009) Response of Mediterranean coralline algae to ocean acidification and elevated temperature. Glob Change Biol 15:2089–2100

Martin S, Castets MD, Clavier J (2006) Primary production, respiration and calcification of the temperate free-living coralline alga *Lithothamnion corallioides.* Aquat Bot 85: 121–128

Martin S, Cohu S, Vignot C, Zimmerman G, Gattuso J (2013) One-year experiment on the physiological response of the Mediterranean crustose coralline alga, *Lithophyllum cabiochae*, to elevated pCO_2 and temperature. Ecol Evol 3:676–693

Martindale W (1992) Calcified epibionts as palaeoecological tools: examples from the Recent and Pleistocene reefs of Barbados. Coral Reefs 11:167–177

Matsuda S (1989) Succession and growth rates of encrusting crustose coralline algae (Rhodophyta, Cryptonemiales) in the upper fore-reef environment off Ishigaki Island, Ryukyu Islands. Coral Reefs 7:185–195

McCoy SJ, Pfister CA (2014) Historical comparisons reveal altered competitive interactions in a guild of crustose coralline algae. Ecol Lett 17:475–483

Montaggioni LF, Cabioch G, Camoin GF, Bard E and others (1997) Continuous record of reef growth over the past 14 k.y. on the mid-Pacific island of Tahiti. Geology 25:555–558

Morgan KM, Kench PS (2017) New rates of Indian Ocean carbonate production by encrusting coral reef calcifiers: Periodic expansions following disturbance influence reef-building and recovery. Mar Geol 390:72–79

Moritz C, Brandl SJ, Rouzé H, Vii J and others (2021) Long-term monitoring of benthic communities reveals spatial determinants of disturbance and recovery dynamics on coral reefs. Mar Ecol Prog Ser 672:141–152

Morse DE, Hooker N, Morse ANC, Jensen RA (1988) Control of larval metamorphosis and recruitment in sympatric agariciid corals. J Exp Mar Biol Ecol 116:193–217

NCBI (National Center for Biotechnology Information) (1988) Basic Local Alignment Search Tool. National Library of Medicine (US), National Center for Biotechnology Information, Bethesda, MD. https://www.ncbi.nlm.nih.gov/ (accessed 2 February 2024)

Nelson WA (2009) Calcified macroalgae—critical to coastal ecosystems and vulnerable to change: a review. Mar Freshw Res 60:787–801

Payri CE (1995) Carbonate production of some calcifying algae in a French Polynesia coral reef. Bull Soc Geol Fr 166:77–84

Payri CE (1997) *Hydrolithon reinboldii* rhodolith distribution, growth and carbon production of a French Polynesian reef. Proc 8th Int Coral Reef Symp 1:755–760

Payri CE (2000) Production primaire et calcification des algues benthiques en milieu corallien. Oceanis 26:427–463

Payri CE, N'Yeurt AR, Orempuller J (2000) Algues de Polynésie Française/Algae of French Polynesia. Au vent des îles, Papeete

Payri CE, Maritorena S, Bizeau C, Rodière M (2001) Photoacclimation in the tropical coralline alga *Hydrolithon onkodes* (Rhodophyta, Corallinaceae) from a French Polynesian reef. J Phycol 37:223–234

Perry CT, Morgan KM (2017) Bleaching drives collapse in reef carbonate budgets and reef growth potential on southern Maldives reefs. Sci Rep 7:40581

Pulecio-Plaza L, Diaz-Pulido G, García-Urueña R (2023) Seasonal upwelling conditions promote growth and calcification in reef-building coralline algae. J Phycol 59:908–925

Rasser M, Riegl B (2002) Holocene coral reef rubble and its binding agents. Coral Reefs 21:57–72

Richter C, Wunsch M, Rasheed M, Kötter I, Badran MI (2001) Endoscopic exploration of Red Sea coral reefs reveals dense populations of cavity-dwelling sponges. Nature 413:726–730

Schubert N, Shoenrock KM, Aguirre J, Kamenos NA, Silva J, Horta PA, Hofman LC (2020) Editorial: Coralline algae: globally distributed ecosystem engineers. Front Mar Sci 7:352

Short J, Kendrick GA, Falter J, McCulloch MT (2014) Interactions between filamentous turf algae and coralline algae are modified under ocean acidification. J Exp Mar Biol Ecol 456:70–77

Short J, Foster T, Falter J, Kendrick GA, McCulloch MT (2015) Crustose coralline algal growth, calcification and mortality following a marine heatwave in Western Australia. Cont Shelf Res 106:38–44

Steller D, Hernandez-Ayón J, Riosmena-Rodríguez R, Cabello-Pasini A (2007) Effect of temperature on photosynthesis, growth and calcification rates of the free-living coralline alga *Lithophyllum margaritae*. Cienc Mar 33: 441–456

Steneck RS (1986) The ecology of coralline algal crusts: convergent patterns and adaptative strategies. Annu Rev Ecol Syst 17:273–303

Steneck RS (1997) Crustose corallines, other algal functional groups, herbivores and sediments: complex interactions along reef productivity gradients. Proc 8th Int Coral Reef Symp 1:695–700

Steneck RS, Adey WH (1976) The role of environment in control of morphology in *Lithophyllum congestum*, a Caribbean algal ridge builder. Bot Mar 19:197–215

Steneck RS, Hacker SD, Dethier MN (1991) Mechanisms of competitive dominance between crustose coralline algae: an herbivore-mediated competitive reversal. Ecology 72: 938–950

Tâmega FTS, Figueiredo MAO (2019) Colonization, growth and productivity of crustose coralline algae in sunlit reefs in the Atlantic southernmost coral reef. Front Mar Sci 6: 81

Tâmega FTS, Figueiredo MAO, Ferreira CEL, Bonaldo RM (2016) Seaweed survival after consumption by the green-beak parrotfish, *Scarus trispinosus.* Coral Reefs 35: 329–334

Tanaka Y, Suzuki A, Sakai K (2017) Effects of elevated seawater temperature and phosphate enrichment on the crustose coralline alga *Porolithon onkodes* (Rhodophyta). Phycol Res 65:51–57

Teichert S, Steinbauer M, Kiessling W (2020) A possible link between coral reef success, crustose coralline algae and the evolution of herbivory. Sci Rep 10:17748

Vásquez-Elizondo RM, Enríquez S (2016) Coralline algal physiology is more adversely affected by elevated temperature than reduced pH. Sci Rep 6:19030

Vermeij MJA, Dailer ML, Smith CM (2011) Crustose coralline algae can suppress macroalgal growth and recruitment on Hawaiian coral reefs. Mar Ecol Prog Ser 422:1–7

Williams SL, Carpenter RC (1990) Photosynthesis/photon flux density relationships among components of coral reef algal turfs. J Phycol 26:36–40

Appendix. Deployment and collection dates and heath and growth measurement of CCA species

Table A1. Deployment and collection dates of PVC rings in both reef habitats. Dates are given as d/mo

		Winter 2021	Spring 2021	Summer 2022	Autumn 2022	Winter 2022
Back reef	Deployment	13/07	19/10/2021	23/01	15/04	22/06
	Collection	15/10	21/01/2022	11/04	22/06	06/10
Fore reef	Deployment	15/07	21/10/2021	25/01	13/04	22/06
	Collection	15/10	21/01/2022	11/04	22/06	06/10

Table A2. Summary of the number of replicates and maximum, minimum, mean and SEM values for the different health, growth and calcification variables for each species × season combination at the (a) back reef and (b) fore reef sites

	P. cf. *onkodes*				*N.* cf. *megalocystum*				*Lithophyllum* sp.			
	n	Max	Mean (SEM)	Min	n	Max	Mean (SEM)	Min	n	Max	Mean (SEM)	Min
(a) Back reef												
Tissue discolouration (% pale tissue area)												
Winter 2021	12	0.00	0.00 (0.00)	0.00	9	35.87	7.34 (3.99)	0.00	9	88.50	10.58 (9.77)	0.00
Spring 2021	12	0.00	0.00 (0.00)	0.00	10	13.42	3.94 (1.67)	0.00	8	2.26	0.28 (0.28)	0.00
Summer 2022	12	0.00	0.00 (0.00)	0.00	10	46.96	6.35 (4.60)	0.00	8	47.76	7.40 (5.94)	0.00
Autumn 2022	11	0.00	0.00 (0.00)	0.00	9	0.00	0.39 (0.39)	0.00	6	17.39	2.90 (2.90)	0.00
Winter 2022	11	1.65	0.15 (0.15)	0.00	11	12.55	1.91 (1.22)	0.00	7	0.00	0.00 (0.00)	0.00
Tissue mortality (% dead tissue area)												
Winter 2021	12	9.18	1.79 (0.82)	0.00	9	18.72	4.50 (2.23)	0.00	9	8.99	1.00 (0.99)	0.00
Spring 2021	12	24.37	3.48 (2.20)	0.00	10	1.97	0.20 (0.20)	0.00	8	47.69	6.83 (5.90)	0.00
Summer 2022	12	18.01	1.76 (1.50)	0.00	10	36.89	5.92 (3.81)	0.00	8	43.75	6.88 (5.45)	0.00
Autumn 2022	11	20.96	3.19 (1.97)	0.00	9	34.15	8.44 (4.27)	0.00	6	28.97	19.80 (13.69)	0.00
Winter 2022	11	15.79	1.66 (1.43)	0.00	11	45.33	4.12 (4.12)	0.00	7	43.89	15.70 (5.90)	0.00
Marginal growth (mm d^{-1})												
Winter 2021	12	0.04	0.015 (0.003)	0.001	9	0.03	0.007 (0.005)	−0.01	9	0.04	0.009 (0.008)	−0.02
Spring 2021	12	0.05	0.019 (0.006)	−0.017	10	0.04	0.012 (0.006)	−0.01	8	0.03	0.012 (0.005)	−0.01
Summer 2022	12	0.09	0.041 (0.008)	−0.01	10	0.01	−0.0001 (0.003)	−0.02	8	0.04	0.008 (0.008)	−0.02
Autumn 2022	11	0.05	0.012 (0.004)	−0.003	9	0.03	0.005 (0.005)	−0.02	6	0.01	0.002 (0.005)	−0.02
Winter 2022	11	0.05	0.03 (0.004)	0.01	11	0.05	0.015 (0.005)	−0.02	7	0.01	0.002 (0.004)	−0.001
Vertical growth (µm d^{-1})												
Winter 2021	12	7.16	4.09 (0.41)	2.03	9	1.54	0.17 (0.17)	0.00	9	2.46	1.37 (0.22)	0.53
Spring 2021	12	6.94	4.69 (0.31)	3.64	10	0.00	0.00 (0.00)	0.00	8	4.32	2.53 (0.60)	0.00
Summer 2022	12	7.61	5.15 (0.34)	2.83	10	7.55	0.75 (0.75)	0.00	8	3.69	0.82 (0.48)	0.00
Autumn 2022	11	5.25	4.35 (0.23)	3.18	9	0.00	0.00 (0.00)	0.00	6	2.72	1.30 (0.49)	0.00
Winter 2022	11	8.89	5.65 (0.48)	3.82	11	0.00	0.00 (0.00)	0.00	7	1.41	0.20 (0.20)	0.00
Net calcification (g $CaCO_3$ cm^{-2} yr^{-1})												
Winter 2021	12	0.80	0.46 (0.05)	0.20	9	0.36	0.08 (0.06)	−0.15	9	0.20	0.02 (0.05)	−0.30
Spring 2021	12	0.81	0.52 (0.04)	0.34	10	0.33	0.10 (0.05)	−0.15	8	0.17	0.07 (0.03)	−0.08
Summer 2022	12	0.86	0.064 (0.05)	0.24	10	0.19	−0.001 (0.05)	−0.29	8	0.19	0.02 (0.05)	−0.17
Autumn 2022	11	0.58	0.46 (0.03)	0.31	9	0.34	0.04 (0.07)	−0.33	6	0.10	−0.03 (0.07)	−0.39
Winter 2022	11	1.13	0.71 (0.06)	0.45	11	0.47	0.17 (0.06)	−0.27	7	0.07	0.02 (0.01)	−0.01

Table continued on next page

Table A2 (continued)

	P. cf. *onkodes*				*N.* cf. *megalocystum*				*Lithophyllum* sp.			
	n	Max	Mean (SEM)	Min	n	Max	Mean (SEM)	Min	n	Max	Mean (SEM)	Min
(b) Fore reef												
Tissue discolouration (% pale tissue area)												
Winter 2021	12	3.89	0.54 (0.37)	0.00	12	5.99	0.50 (0.50)	0.00	6	0.00	0.00 (0.00)	0.00
Spring 2021	12	0.00	0.00 (0.00)	0.00	12	21.54	1.80 (1.80)	0.00	10	0.00	0.00 (0.00)	0.00
Summer 2022	12	0.00	0.00 (0.00)	0.00	12	8.52	0.71 (0.71)	0.00	10	45.19	4.52 (4.52)	0.00
Autumn 2022	12	9.75	0.81 (0.81)	0.00	12	9.54	0.79 (0.79)	0.00	11	0.00	0.00 (0.00)	0.00
Winter 2022	11	3.29	0.30 (0.30)	0.00	11	0.00	0.00 (0.00)	0.00	7	0.00	0.00 (0.00)	0.00
Tissue mortality (% dead tissue area)												
Winter 2021	12	33.14	4.86 (2.96)	0.00	12	4.27	0.64 (0.44)	0.00	6	38.53	7.31 (6.30)	0.00
Spring 2021	12	0.00	0.00 (0.00)	0.00	12	4.61	0.56 (0.41)	0.00	10	14.74	5.04 (1.87)	0.00
Summer 2022	12	0.00	0.00 (0.00)	0.00	12	11.68	2.27 (1.12)	0.00	10	22.93	6.56 (2.76)	0.00
Autumn 2022	12	14.71	2.07 (1.34)	0.00	12	5.70	0.48 (0.48)	0.00	11	39.56	5.95 (4.04)	0.00
Winter 2022	11	47.35	5.88 (4.32)	0.00	11	26.25	2.94 (2.40)	0.00	7	56.67	14.83 (7.64)	0.00
Marginal growth (mm d^{-1})												
Winter 2021	12	0.04	0.018 (0.006)	−0.01	12	0.08	0.041 (0.008)	0.001	6	0.04	0.003 (0.004)	−0.01
Spring 2021	12	0.07	0.052 (0.004)	0.03	12	0.09	0.043 (0.006)	0.013	10	0.02	0.005 (0.003)	−0.01
Summer 2022	12	0.10	0.051 (0.007)	0.02	12	0.06	0.025 (0.006)	0.003	10	0.16	0.033 (0.002)	−0.01
Autumn 2022	12	0.10	0.046 (0.008)	0.01	12	0.07	0.032 (0.006)	0.001	11	0.05	0.012 (0.006)	−0.01
Winter 2022	11	0.09	0.048 (0.009)	−0.02	11	0.18	0.080 (0.017)	0.02	7	0.17	0.034 (0.023)	−0.01
Vertical growth (µm d^{-1})												
Winter 2021	12	3.81	3.14 (0.22)	1.41	12	1.63	0.14 (0.14)	0.00	6	2.26	0.85 (0.31)	0.00
Spring 2021	12	6.99	3.91 (0.51)	0.00	12	0.00	0.00 (0.00)	0.00	10	2.77	1.09 (0.27)	0.00
Summer 2022	12	9.90	5.59 (0.56)	2.07	12	0.00	0.00 (0.00)	0.00	10	2.56	1.17 (0.30)	0.00
Autumn 2022	12	9.92	5.25 (0.52)	3.76	12	0.00	0.00 (0.00)	0.00	11	3.22	0.89 (0.36)	0.00
Winter 2022	11	7.71	5.72 (0.49)	3.48	11	0.00	0.00 (0.00)	0.00	7	3.39	0.74 (0.50)	0.00
Net calcification (g $CaCO_3$ cm^{-2} yr^{-1})												
Winter 2021	12	0.49	0.34 (0.03)	0.17	12	0.57	0.33 (0.05)	0.02	6	0.10	0.006 (0.03)	−0.12
Spring 2021	12	0.95	0.53 (0.07)	0.00	12	0.57	0.34 (0.04)	0.17	10	0.11	0.03 (0.02)	−0.06
Summer 2022	12	1.21	0.71 (0.07)	0.30	12	0.51	0.25 (0.05)	0.05	10	0.35	0.09 (0.05)	−0.16
Autumn 2022	12	1.24	0.65 (0.06)	0.38	12	0.66	0.30 (0.06)	0.01	11	0.22	0.05 (0.03)	−0.17
Winter 2022	11	1.13	0.80 (0.07)	0.48	11	0.63	0.45 (0.05)	0.20	7	0.26	0.07 (0.04)	−0.07

Editorial responsibility: Chris Langdon, Coral Gables, Florida, USA
Reviewed by: J. Mallela, G. Diaz-Pulido and 1 anonymous referee

Submitted: February 28, 2024
Accepted: May 16, 2024
Proofs received from author(s): June 27, 2024